

Two-Nucleon Emission Following Absorption of Stopped Negative Pions*

M. E. NORDBERG, JR.,† K. F. KINSEY,‡ AND R. L. BURMAN

Department of Physics and Astronomy, University of Rochester, Rochester, New York

(Received 7 August 1967)

A beam of π^- was brought to rest in a variety of light-element targets. The angular distributions of nucleon pairs emitted in the subsequent pion absorption were measured. The angular distributions peak strongly at 180° , supporting the two-nucleon model of the absorption process. The emission of an n - p (n - n) pair implies capture of the π^- by a p - p (n - p) pair inside the nucleus. The ratio of n - n to n - p emission has been measured to be 3.3 ± 0.9 averaged over p -shell nuclei. This is compared with predictions of this ratio which are sensitive to the two-nucleon correlation within the nucleus. Measurements of the proton spectra have been made in the n - p emission and are in agreement with the two-nucleon mechanism. The branching ratio of π^- absorption yielding two correlated nucleons is typically 40%.

I. INTRODUCTION

THE mechanism of stopped π^- absorption on complex nuclei is still little understood. Since the early theory of Brueckner, Serber, and Watson¹ of a phenomenological extrapolation of capture on deuterium, many theoretical refinements to such a two-nucleon capture mechanism have been made.²⁻¹⁴ Other absorption mechanisms have also been calculated^{5,12,15-19}

and measured,²⁰⁻²⁶ but the sparse data have in general not allowed definitive statements of their relative importance. This experiment was designed to shed some light on the absorption process, especially the two-nucleon capture process, through the detection of two correlated nucleons following stopped π^- absorption. However, caution must be exercised in forming conclusions from an experiment of this sort, since the detection of two nucleons in coincidence may inherently bias the experiment against some of the other absorption mechanisms.

A detailed description of π^- absorption leading to two-nucleon emission requires the knowledge of six independent kinematical variables to specify a definite three-body final state. Assumptions about the form of the interaction lead to theoretical calculations involving fewer variables; in particular, several theorists predict distributions in the variables \mathbf{K} , \mathbf{k} , and θ (the momentum sum of the two nucleons, half the momentum difference, and the angle between these momenta) as defined in Fig. 1. We have not measured the requisite number of variables to completely determine a three-body final state. Instead, we have measured the distribution in ψ (the laboratory angle between the two nucleons), and in \mathbf{k} (the momentum of a single nucleon) for the emission of a proton-neutron pair only. These distributions are in large part determined by the kinematical requirements of conservation of energy and momentum. We have also measured the ratio of the probability of

* Supported in part by the U. S. Atomic Energy Commission and the National Science Foundation.

† Present address: Laboratory of Nuclear Studies, Cornell University, Ithaca, N. Y. 14850.

‡ Present address: Department of Physics, State University of New York, Geneseo, N. Y.

¹ K. A. Brueckner, R. Serber, and K. M. Watson, *Phys. Rev.* **84**, 258 (1951).

² P. Ammiraju and S. N. Biswas, *Nuovo Cimento* **17**, 726 (1960).

³ P. Huguenin, *Z. Physik* **167**, 416 (1962).

⁴ T. Ericson, *Phys. Letters* **2**, 278 (1962); T. E. O. Ericson, in *Proceedings of the International Conference on Nuclear Physics, Gallatinburg, Tennessee, 1966* (Academic Press, Inc., New York, 1967).

⁵ S. G. Eckstein, *Phys. Rev.* **129**, B413 (1963).

⁶ R. I. Jibuti and T. I. Kopaleishvili, *Nucl. Phys.* **55**, 337 (1964).

⁷ I. T. Cheon, Y. Sakamoto, and C. Nguyen-Trung, *Progr. Theoret. Phys. (Kyoto)* **34**, 574 (1965); Il-Tong Cheon, *Phys. Rev.* **145**, 794 (1966); Il-Tong Cheon, *ibid.* **158**, 900 (1967).

⁸ P. D. Divarkaran, *Phys. Rev.* **139**, B387 (1965).

⁹ T. Kohmura, *Progr. Theoret. Phys. (Kyoto)* **34**, 234 (1965).

¹⁰ T. I. Kopaleishvili, *Yadern. Fiz.* **1**, 961 (1965) [English transl.: *Soviet J. Nucl. Phys.* **1**, 686 (1965)]; T. I. Kopaleishvili, I. Z. Machabeli, G. Sh. Godsadze, and N. B. Krupennikova, *Phys. Letters* **22**, 181 (1966); T. I. Kopaleishvili, *Yadern. Fiz.* **4**, 538 (1966) [English transl.: *Soviet J. Nucl. Phys.* **4**, 382 (1967)]; T. I. Kopaleishvili, *Nucl. Phys.* **B1**, 335 (1967).

¹¹ Y. Sakamoto, *Nuovo Cimento* **37**, 774 (1965); Y. Sakamoto and I. T. Cheon, *Progr. Theoret. Phys. (Kyoto)* **34**, 814 (1965); C. Nguyen-Trung and Y. Sakamoto, *Nucl. Phys.* **B1**, 139 (1967).

¹² V. M. Kolibasov, Institute for Theoretical and Experimental Physics, Moscow, Report No. 376, 1966 (unpublished).

¹³ D. S. Koltun and A. Reitan, *Phys. Rev.* **141**, 1413 (1966); D. S. Koltun, *ibid.* **162**, 963 (1967); D. S. Koltun and A. Reitan, *ibid.* **155**, 1139 (1967).

¹⁴ J. M. Eisenberg and J. LeTourneux, *Nucl. Phys.* **B3**, 47 (1967).

¹⁵ R. M. Spector, *Phys. Rev.* **134**, B101 (1964).

¹⁶ O. A. Zaimidoroga, M. M. Kulyukin, R. M. Solyaev, I. V. Fulomkin, A. I. Filippou, V. M. Tsupko-Sitnikov, and Yu. A. Shcherbakov, *Zh. Eksperim. i Teor. Fiz.* **48**, 1267 (1965) [English transl.: *Soviet Phys.—JETP* **21**, 848 (1965)].

¹⁷ D. K. Anderson and J. M. Eisenberg, *Phys. Letters* **22**, 164 (1966).

¹⁸ T. I. Kopaleishvili and I. Z. Machabeli, *Yadern. Fiz.* **4**, 37 (1966) [English transl.: *Soviet J. Nucl. Phys.* **4**, 27 (1967)].

¹⁹ J. LeTourneux and J. M. Eisenberg, *Nucl. Phys.* **87**, 331 (1966); J. LeTourneux, *Nucl. Phys.* **81**, 665 (1966).

²⁰ F. H. Tenney and J. Tinlot, *Phys. Rev.* **92**, 974 (1953).

²¹ P. Ammiraju and L. M. Lederman, *Nuovo Cimento* **4**, 283 (1956).

²² M. Schiff, R. H. Hildebrand, and C. Giese, *Phys. Rev.* **122**, 265 (1961).

²³ A. T. Varfolomeev, *Zh. Eksperim. i Teor. Fiz.* **42**, 713 (1962) [English transl.: *Soviet Phys.—JETP* **15**, 496 (1962)].

²⁴ A. O. Vaisenberg, E. D. Kolgova, and N. V. Rabin, *Zh. Eksperim. i Teor. Fiz.* **47**, 1262 (1964) [English transl.: *Soviet Phys.—JETP* **20**, 854 (1965)].

²⁵ R. C. Cohen, A. D. Kanaris, S. Margulies, and J. L. Rosen, *Phys. Letters* **14**, 242 (1965).

²⁶ H. Davies, H. Muirhead, and J. N. Wouds, *Nucl. Phys.* **78**, 673 (1966).

emission of two neutrons to the emission of a neutron and proton: $R = W(n-n)/W(n-p)$. This ratio is hopefully somewhat sensitive to the two-nucleon correlations within the target nucleus.

Early experiments^{21-24,27-31} of π^- absorption in cloud chambers, emulsions, and bubble chambers were insensitive to neutrons. In fact, most processes of π^- capture emit at least one fast neutron. Ozaki *et al.*³² have measured $R = 5 \pm 1.5$ in C and 3.9 ± 1.2 in Al, with most of the nucleon pairs having been emitted back-to-back. An elegant experiment by Davies *et al.*³³ has used time-of-flight techniques to measure the energies of the two neutrons in the process $\text{Li}^6(\pi^-, n)n\text{He}^4$. We have used an apparatus similar to that of Ozaki *et al.*³² with much improved angular resolution to obtain angular distributions of the two-nucleon emission following π^- absorption in a number of p -shell nuclei, Al, Cu, and Pb targets. The angular distributions were integrated to obtain the absolute value of correlated emission of $n-n$ and $n-p$ pairs. Their ratio and also the observed proton energy distribution in $n-p$ emission are compared to theories. A preliminary report of this work is contained in Ref. 34.

II. EXPERIMENTAL ARRANGEMENT

A. Apparatus

The π^- beam was extracted from the Rochester 130-in. cyclotron at an energy of 32 MeV and an energy spread of $\pm 10\%$. It was focused by the fringe field of the cyclotron and then bent 60° by a double-focusing magnet into a large iron box which shielded the photomultipliers from the main magnet's fringe field. The cyclotron was operated with a "Cee" to give a stretched duty cycle of about 75%. This was crucial to reduce random coincidences to a tolerable level although the beam intensity of $4 \times 10^3/\text{sec}$ was only $\frac{2}{3}$ the "prompt" intensity available. About half of the beam stopped in

²⁷ M. Demeur, A. Huleux, and G. Vanderhaeghe, *Nuovo Cimento* **4**, 509 (1956).

²⁸ S. A. Azimov, U. G. Guliamov, E. A. Zamchalova, M. Nizametdinova, M. I. Podgoretskii, and A. Iuldashev, *Zh. Eksperim. i Teor. Fiz.* **31**, 756 (1956) [English transl.: *Soviet Phys.—JETP* **4**, 632 (1957)].

²⁹ V. S. Demidov, V. G. Kirillov-Ugryumov, A. K. Ponosov, V. P. Protasov, and F. M. Sergeev, *Zh. Eksperim. i Teor. Fiz.* **44**, 1144 (1963) [English transl.: *Soviet Phys.—JETP* **17**, 773 (1963)]; V. S. Demidov, V. S. Verebryusov, V. G. Kirillov-Ugryumov, A. K. Ponosov, and F. M. Sergeev, *Zh. Eksperim. i Teor. Fiz.* **46**, 1220 (1964) [English transl.: *Soviet Phys.—JETP* **19**, 826 (1964)].

³⁰ P. I. Fedotov, *Yadern. Fiz.* **2**, 466 (1965) [English transl.: *Soviet J. Nucl. Phys.* **2**, 235 (1966)].

³¹ P. H. Fowler, *Proc. Phys. Soc. (London)* **85**, 1051 (1965).

³² S. Ozaki, R. Weinstein, G. Glass, E. Loh, L. Neimala, and A. Wattenberg, *Phys. Rev. Letters* **4**, 533 (1960).

³³ H. Davies, H. Muirhead, and J. N. Woulds, *Nucl. Phys.* **78**, 663 (1966).

³⁴ R. L. Burman, K. F. Kinsey, and M. E. Nordberg, *Bull. Am. Phys. Soc.* **10**, 36 (1965); M. E. Nordberg, Jr., K. F. Kinsey, and R. L. Burman, in *Proceedings of the Williamsburg Conference on Intermediate Energy Physics, Williamsburg, 1966* (unpublished).

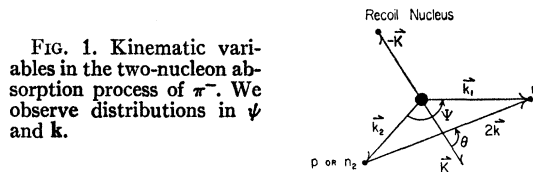


FIG. 1. Kinematic variables in the two-nucleon absorption process of π^- . We observe distributions in ψ and θ .

the target (typically 0.5 g/cm^2 thick), with the absorber optimized.

Two sets of apparatus were used to collect most of the data. Both employed plastic scintillation detectors to detect pions, neutrons, and protons. One set had large detectors close to the target and therefore a poor angular resolution. It was used with all target materials to determine the ratios R . A second apparatus had smaller detectors with finer angular resolution and was used to determine the detailed angular distributions with Li^6 and O^{16} targets.

The apparatus with larger detectors is shown in Fig. 2. A stopped pion was detected by coincidence signals from π_a , π_b , and not π_c . Protons were detected as a coincidence in P_a and P_b . The pulse height in P_b , made of $1\frac{1}{2}$ -in.-thick plastic scintillator, could be recorded as a measure of the proton energy. The target was placed normal to the proton detector in order to minimize the proton energy loss in the target. Neutrons were detected in the 3-in.-diam \times 6-in.-long cylinders of plastic scintillator. These were placed inside and behind anticoincidence guard detectors which vetoed any charged particles originating from the target or from the background. The detectors were enclosed in cylindrical shields of lead and steel.

The logic circuitry was cabled so that three angles of $p-n$ coincidences and three angles of $n-n$ coincidences as well as the respective randoms were counted simultaneously. Counting rates were typically 40 counts/h for each pair of detectors, with a random contribution of about 15% for the neutron-neutron detector pairs and about 3% for the proton-proton detector pairs. For those data when the proton pulse height was also recorded, the storage of this pulse height was routed into a separate subsection of a 400-channel analyzer for each neutron detector.

The apparatus with the smaller neutron detectors is shown in Fig. 3. A stopped pion was recorded as before. Three proton telescopes were used in this case. They were made of one common front scintillator followed by disks of scintillator of the same area as a neutron detector. The energy of the protons could not be recorded with this apparatus. The neutron detectors were 2-in.-diam \times 4-in.-long cylinders of plastic scintillator. They were covered by an anticoincidence detector on the end toward the target but not on the surrounding sides since little of the background was reduced by such shields in the previous case.

For the case of Fig. 3, the logic circuits formed coincidences of all nine possible $n-p$ pairs which were also in coincidence with a stopped pion. Background

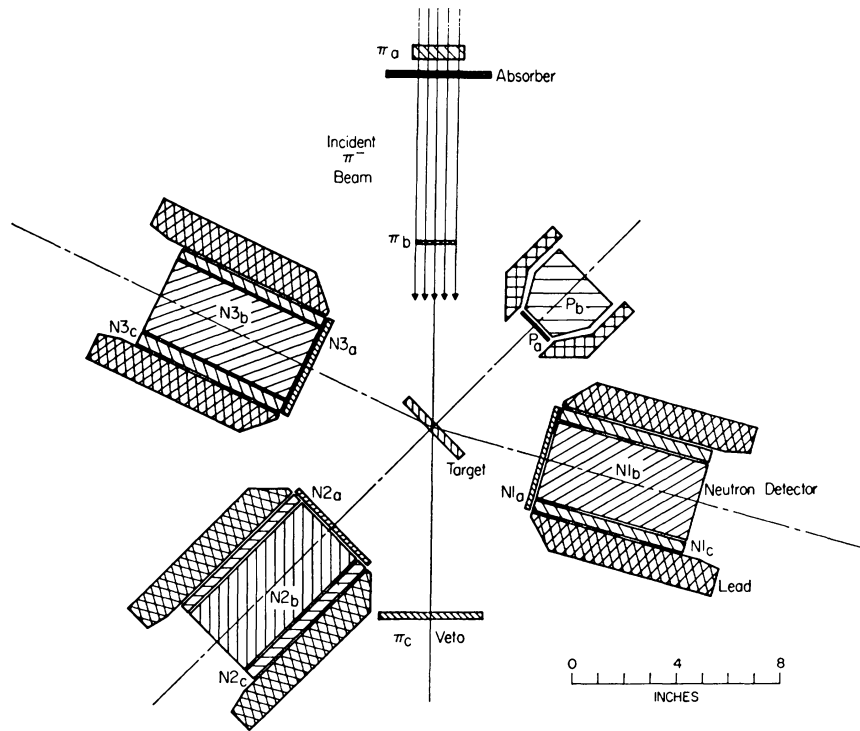


FIG. 2. Apparatus of coarser angular resolution for detection of p - n and n - n pairs following π^- absorption.

was measured by removing the target but it was very small. The fine resolution n - n data was collected with a fourth neutron detector in place of the proton detectors. All six pairs of n - n coincidences were recorded. Counting rates were typically 5 to 10 counts/h for each pair of detectors.

The intensity profile of the pion beam was recorded across the face of the target. With a numerical integration procedure this profile was folded together with the acceptance solid angles of the proton telescope and neutron detector, or two neutron detectors, in order to determine the resolution function of the apparatus. The full width at half-maximum height of these resolution functions is about 26° for the first apparatus and 13° for the second. Since the solid-angle factor is proportional to $\sin\psi$, the peak in the resolution function occurs at a smaller angle than the nominal laboratory angle between detectors; this effect is most noticeable at 180° . The main use of the resolution functions was to find the centroid for each pair of detector positions. The data are plotted at those centroid angles. In addition, the resolution was folded together with theoretical predictions to compare with the data as explained in Sec. III.

B. Detector Efficiencies

In order to have a high detection efficiency the discriminator bias on the larger neutron detectors was set low (a pulse height corresponding to 6.5-MeV protons). This threshold was calibrated by comparison with the pulse height produced by 5-MeV capture γ rays in the

$C^{12}(n,\gamma)C^{13}$ reaction from the background flux of thermal neutrons and also by comparison with conversion electrons from a Bi^{207} source. For the smaller detectors a bias corresponding to 10.5-MeV protons was set.

The efficiencies of the plastic scintillator neutron detectors were calculated in a manner similar to that employed by Swartz *et al.*³⁵ and by Bowen *et al.*³⁶ Single and double scattering of neutrons by the hydrogen and carbon in the scintillator, and reactions of neutrons in the carbon, were considered along with an approximate treatment of edge and end effects due to finite counter geometry. The calculated neutron efficiencies are shown in Fig. 4; the error in the calculation is estimated to be $\pm 15\%$. The uncertainties in the efficiencies have only a minor effect on the proton spectra or the nucleon-nucleon angular correlations but a major effect on the absolute values of $W(n-n)$ and $W(n-p)$ and on their ratio.

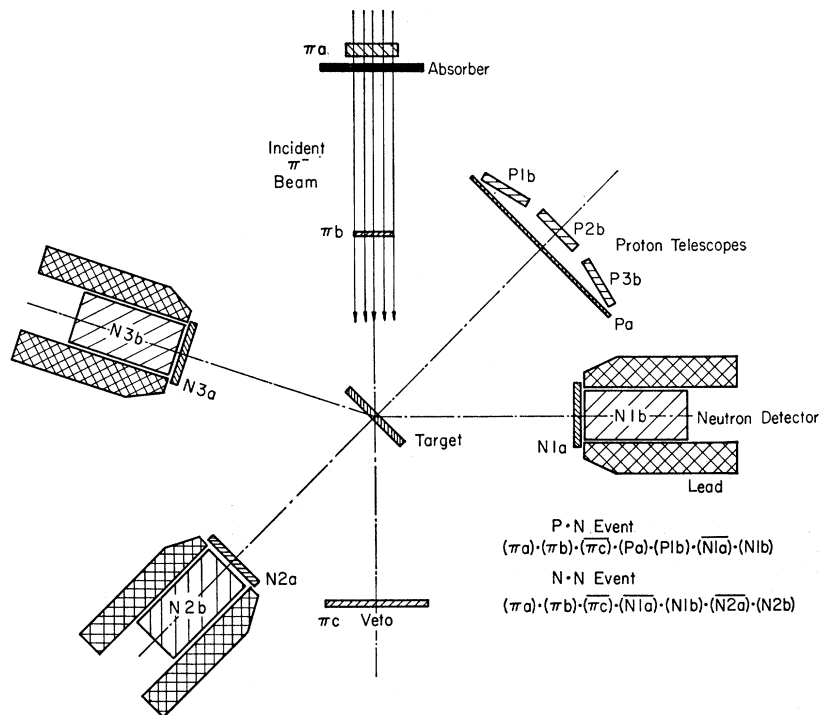
In order to ensure that we were seeing a direct two-nucleon emission process, it was essential that we did not detect the large number of low-energy nucleons produced by an evaporation mechanism following the π^- absorption. Anderson *et al.*³⁷ have shown that the evaporation mechanism is negligible for neutrons with energies larger than 20 MeV. Since neutrons with energies less than 20 MeV were discriminated against by

³⁵ C. D. Swartz, G. E. Owen, and O. Armes, John Hopkins University Report No. NVO-2053, 1957 (unpublished).

³⁶ P. H. Bowen, G. C. Cox, G. B. Huxtable, A. Langsford, J. P. Scanlon, G. H. Stafford, and J. J. Thresher, Nucl. Instr. Methods **17**, 117 (1962).

³⁷ H. L. Anderson, E. P. Hincks, C. S. Johnson, C. Rey, and A. M. Segar, Phys. Rev. **133**, B392 (1964).

FIG. 3. Apparatus of finer angular resolution for detection of p - n and n - n pairs following π^- absorption.



the high bias levels used on our detectors, as can be seen in the efficiency curves of Fig. 4, while protons with energies less than about 20 MeV were nearly all stopped in the target or the first element of the proton telescope, our detection system was largely insensitive to evaporation nucleons.

The pulse-height response of the proton detector was calibrated by comparison of the spectrum with that of a different detector made up of three scintillators: a thin scintillator, followed by a second detector $1\frac{1}{2}$ in. (4 g/cm^2) thick in which we measure the pulse height, followed by another thin scintillator. Since it was found that only a very small number of protons traveled completely through the three-counter telescope, the shape of the energy spectra in the thick detectors of the two telescopes was assumed to be the same. The pulse-height peak seen in the thick detector of the three-counter telescope when operated in threefold coincidence corresponded to about 75 MeV and its position was used to calibrate the proton detector. This method is more accurate than checks of low-energy α -particle or electron sources which were also performed, and is probably in error by less than 10%.

The over-all efficiency of detection of protons depends on target thickness, the thickness of the first element of the proton telescope, the inherent scintillation detector efficiency, and the energy spectrum of the protons. As calculated with the theoretical spectrum of curves (b) in Fig. 5 or Fig. 6, described below, this efficiency was about 98%. With the phase-space curves (a), it was about 90%. We have used 95% in the calculations, with an estimated error of $\pm 5\%$.

Products of the effective solid angles of pairs of detectors were determined in the calculation of the resolution functions of each apparatus. These were: $\Omega_{n1} \times \Omega_{n2} = 0.011$ and $\Omega_p \times \Omega_n = 0.0049$ for the larger detectors and $\Omega_{n1} \times \Omega_{n2} = 0.0011$ and $\Omega_p \times \Omega_n = 0.00104$ for the smaller detectors. The uncertainty in these numbers is small and was neglected.

III. RESULTS AND DISCUSSION

A. Proton Spectra

The pulse-height spectra of protons in coincidence with neutrons is shown in Fig. 5 for a C^{12} target and in

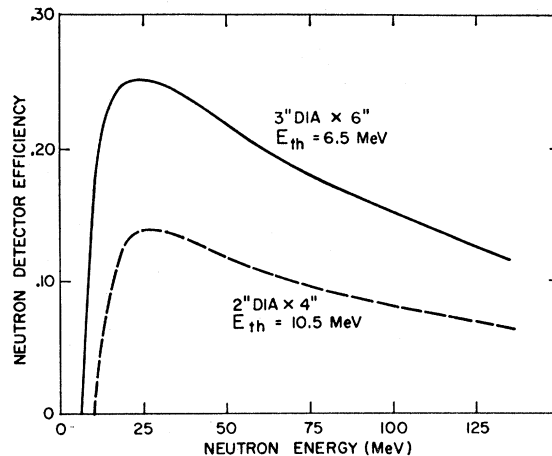


FIG. 4. Calculated neutron detection efficiencies.

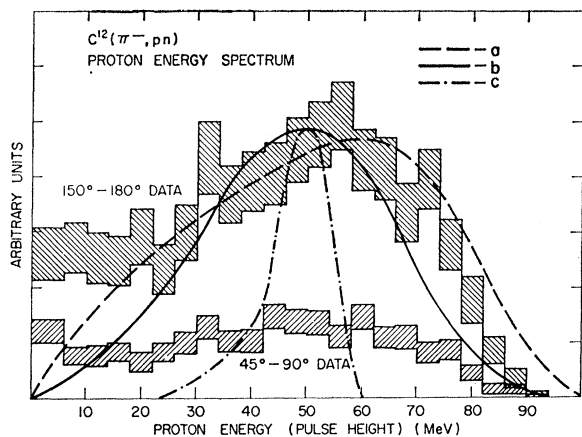


FIG. 5. Proton energy spectra from the pulse height in detector P_b for coincidences with a neutron and stopped pion for a C^{12} target. The curves are obtained by integrating expression (1), taken from Koltun and Reitan (Ref. 13), over unmeasured variables. Curve (a) is a phase-space calculation with the harmonic-oscillator strength parameter $\beta = \infty$, curve (b) is for $\beta = 1.6 F$, and curve (c) is for $\beta = 0$.

Fig. 6 for an O^{16} target. The data are represented by histograms of which the shaded part represents the statistical errors.

Also on each figure three calculated curves are drawn. These are derived from the analytic expression of Koltun and Reitan.¹³

$$\frac{\partial^2 W(k, y)}{\partial K \partial y} \propto \frac{K(k^2 - \frac{1}{4}K^2)^2 \sum |M|^2}{y^2 [(k^2 + \frac{1}{4}K^2)^2 y^2 - (k^2 - \frac{1}{4}K^2)^2]^{1/2}}, \quad (1)$$

where $y = \cos\psi$, k and K are the magnitudes of the momenta as in Fig. 1, and $\sum |M|^2$ is the matrix element. We have assumed $\sum |M|^2$ is independent of $z = \cos\theta$ and can be approximated by a gaussian in K as in Ref. 13:

$$\sum |M|^2 \propto e^{-K^2 \beta^2 A}, \quad (2)$$

where β is the harmonic-oscillator strength parameter and A is a recoil effect. The relative and c. m. momenta are related by the energy equation:

$$k^2 + \frac{1}{2}(\frac{1}{2} + M_n/M_{\text{daughter}})K^2 = M_n[M_\pi + M_{\text{target}} - (M_{\text{daughter}} + 2M_n)]. \quad (3)$$

The probabilities suggested by Kopaleishvili¹⁰ of capture on two nucleons in the p shell, one in the p and one in the s shell, and two in the s shell (taken as 70, 15, and 15%, respectively) are accounted for by adding energies of 0, 13, and 26 MeV to the value of M_{daughter} . The expression (1) is converted to the variables k_p , K , and ψ and integrated over all angles greater than 150° and allowed values of K . Also, folded into this integral, are the pulse-height resolution of the proton detector, the energy loss in the target and first element of the proton telescope, and the neutron detection efficiency.

Curve (a) is a phase-space calculation proportional to the product of the proton and neutron kinetic energies

and the experimental neutron detection efficiency. It is equivalent to the assumption that the matrix element is independent of K (i.e., $\beta = \infty$). It predicts somewhat of an excess of high-energy protons. Curves (b) use a value of $\beta = 1.6 F$ for C^{12} and $1.75 F$ for O^{16} in the matrix element. Curve (c) is a similar calculation assuming the matrix element to be a δ function at $K = 0$, i.e., assuming equal sharing of the available energy between the two nucleons and $\beta = 0$. It represents the response of the apparatus.

It is clear that curves (b) reasonably well reproduce the data except at low energy. Experimentally there is an excess of low-energy protons. These are probably related to the small isotropic component in the angular distribution as shown by the flatness of the 45° - 90° data compared to the 180° data.

The recent calculation of the two-nucleon capture mechanism by Eisenberg and LeTourneur¹⁴ also gives the energy spectra of one nucleon in two-nucleon emission after π^- absorption on O^{16} . Their calculations consider the atomic pion wave function, the relative spin and correlations of the two nucleons within the nucleus, and the final-state interaction. Our observed spectrum shape is in agreement with many of their calculated curves. However, we are unable to test their prediction that under certain conditions there will be a dip in the energy spectrum due to the final-state interaction.

This measurement of only one of the nucleon energies, although it is in coincidence with another nucleon, is not as sensitive a test of various two-nucleon matrix elements as would be the measurement of both energies. The disagreement with the phase-space curves is not severe and if the energy calibration were in error by as much as 15%, they would nearly be in agreement. However, as a test of the two-nucleon mechanism versus other capture processes, the spectra are in reasonable agreement with the two-nucleon process.

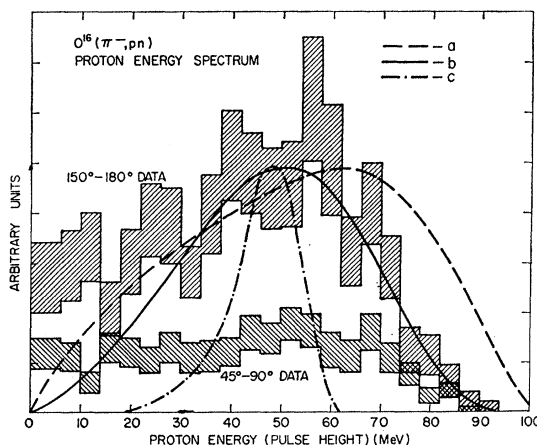


FIG. 6. Proton energy spectra from the pulse height in detector P_b coincidences with a neutron and stopped pion for an O^{16} target. The curves are obtained as in Fig. 5 with $\beta = \infty$, $\beta = 1.75 F$, and $\beta = 0$.

The absolute rates of our measure p - n emission indicate that a major fraction of all high-energy protons emitted in π^- capture are accompanied by a neutron. Fowler's data on the proton spectra from oxygen in emulsion give an absolute rate of 0.075 protons above 60 MeV per captured pion.³¹ From our data the fraction of protons above 60 MeV (above 55 MeV in Figs. 5 and 6) are 35 and 30% of the total for C^{12} or O^{16} . When multiplied by the $W(p-n)$ absolute rate for correlated and isotropic emission, these give about 0.065 protons above 60 MeV accompanied by a neutron per captured pion. In another emulsion experiment, Vaisenberg²⁴ erroneously concluded that the two-nucleon mechanism is not present at all from data similar to Fowler's of a few percent emission of protons over 60 MeV.

B. Angular Correlations

Our data taken with the apparatus of finer resolution are shown in Figs. 7 and 8. Figure 7 shows the relative number of n - n coincidences and Fig. 8 the relative number of p - n coincidences as a function of the angle. The resolution function of the apparatus is shown at one point. The vertical scale is arbitrary but is the same for the Li^6 and O^{16} data. Note that the p - n peak is clearly wider than the corresponding n - n peak in the data for Li^6 . This feature also appeared for most of the targets in the data taken with the coarser resolution. It affects as a matter of definition the determination of the ratio of correlated emission as discussed more fully later.

The data taken on many elements with the apparatus of coarser resolution show a general monotonic decrease in rate as the atomic weight increases. These data have been fitted with an arbitrary function made up of a constant plus an exponential of variable width plus a gaussian of variable width. The exponential plus gaussian parts of the peaks, multiplied by the solid angle, were integrated to give what we call the correlated emission rate: $W(n-n)$ or $W(n-p)$ as listed in Table I.

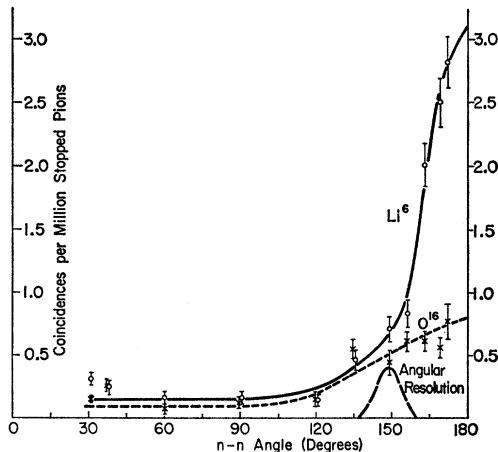


FIG. 7. Angular distribution of n - n emission from targets of Li^6 and O^{16} as measured with apparatus with the finer resolution.

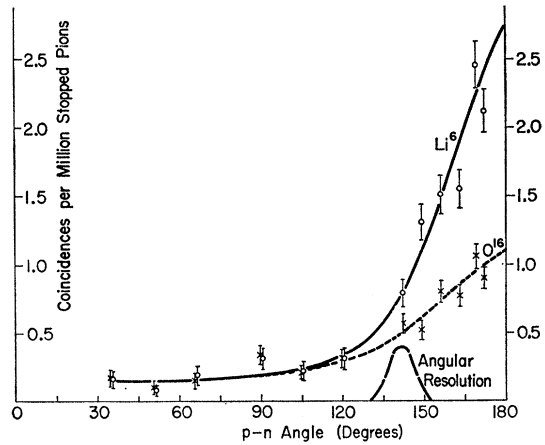


FIG. 8. Angular distribution of p - n emission from targets of Li^6 and O^{16} as measured with apparatus with the finer resolution.

For the p -shell nuclei, $W(n-n)$ averages to about 0.30 and $W(n-p)$ to about 0.10. Thus a sizeable fraction, about 40%, of the stopped π^- absorption events lead to a 180° -correlated emission of two nucleons. The isotropic component from the data analyses, when integrated over all solid angles, is an average of 1.1 times the correlated rate for $W(n-n)$ and 1.3 times the correlated rate for $W(n-p)$. This experiment is not, however, capable of yielding the relative amounts of single, double, and multiple nucleon emission per stopped pion.

The same data for the angular correlation of both n - p pairs and n - n pairs from Li^6 and O^{16} are shown in Figs. 9 and 10 renormalized to the same peak height at 180° as also are the theoretical curves. To look for agreement one must compare the shape of curves versus data.

In both cases the solid curve represents the correlation predicted by expression (1)¹³ with an additional isotropic contribution added. For each value of y , expression (1) is integrated over all allowed values of K , again folding in the pulse-height resolution, energy loss,

TABLE I. Number of correlated emissions per stopped pion and ratio.

Target	$W(n-n)$	$W(n-p)$	Ratio $W(n-n)/W(n-p)$
Li^6	0.41 ± 0.17	0.11 ± 0.03	3.7 ± 1.0
Li^6 ^a	0.69 ± 0.28	0.23 ± 0.06	3.0 ± 0.8
Li^7	0.50 ± 0.21	0.13 ± 0.04	3.7 ± 1.0
Be^9	0.33 ± 0.13	0.10 ± 0.02	3.3 ± 0.9
B^{10}	0.19 ± 0.08	0.08 ± 0.02	2.3 ± 0.8
B^{11}	0.23 ± 0.10	0.05 ± 0.01	4.4 ± 1.3
C^{12}	0.14 ± 0.06	0.06 ± 0.02	2.5 ± 1.0
N^{14}	0.14 ± 0.06	0.04 ± 0.01	3.7 ± 1.1
O^{16}	0.27 ± 0.11	0.08 ± 0.02	3.4 ± 1.1
O^{16} ^a	0.39 ± 0.16	0.10 ± 0.03	3.8 ± 1.0
Al^{27}	0.07 ± 0.03	0.03 ± 0.01	2.4 ± 0.9
Cu	0.08 ± 0.05	0.04 ± 0.01	2.0 ± 1.4
Pb	0.06 ± 0.06	0.01 ± 0.01	4.7 ± 4.7

Weighted average of p -shell nuclei 3.3 ± 0.9
(Weighted average of ratio at 180° 5.1 ± 1.6)

^a Data taken with apparatus of finer angular resolution.

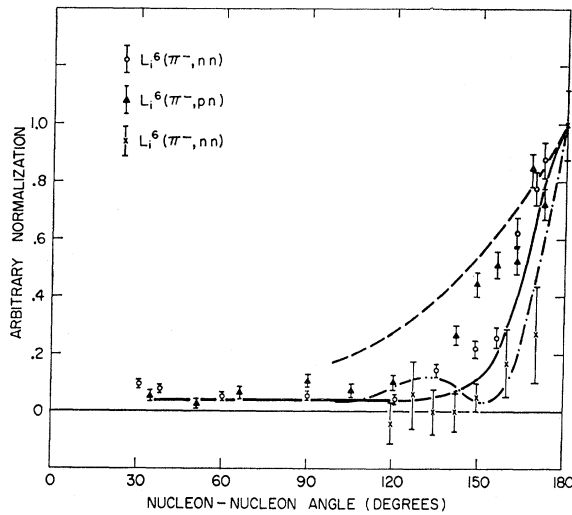


FIG. 9. Angular distribution from Li^6 compared with theories. All data and theories have been normalized to 1.0 at 180° . The data labeled with \times are from Davies *et al.* (Ref. 33) and represent He^4 left in the ground state. The solid curve is an integration of expression (1) taken from Koltun and Reitan (Ref. 13), integrated over unmeasured variables. The dash curve is a shell-model calculation from Kopaleishvili and Machabeli (Ref. 18), and the dot-dashed curve is their calculation for an α - d model of Li^6 .

detection efficiency and angular resolution of the apparatus. Values of the harmonic-oscillator parameter of $\beta=2.2$ F for Li^6 and $\beta=1.75$ F for O^{16} were used in the matrix element in this prediction. Also, the same percentages predicted by Kopaleishvili¹⁰ of the π^- absorption occurring in the p shell, the s and p shells, and the s shell are used in the kinematics. The resolution of our apparatus was folded into this theoretical curve rather than correcting the data for resolution but this does not broaden the curve significantly.

Two features are apparent in these comparisons: (1) the width of the p - n peak is broader than the width of the n - n peak. This is so far completely unexplained but the effect occurs in nearly all the cases we have studied and is probably not instrumental. (2) The data exhibit broader curves than this calculation. This could be due to the interactions of the outgoing nucleons with the residual nucleus or with each other, neither of which is taken into account in this theory. Also shown in Fig. 9 are the data of Davies *et al.*³³ for which they have selected events leaving the He^4 recoil nucleus in the ground state. Their data are significantly narrower than ours and do not show as much isotropic contribution.

Kopaleishvili has calculated¹⁸ the $\text{Li}^6(\pi^-,nn)\text{He}^4$ angular distributions on the basis of an α - d model, the shell model, and a 3-particle model of Li^6 . The dash curve in Fig. 9 is his shell-model calculation. The 3-particle model lies even further from the data. His α - d model calculation is shown by the dot-dashed curve and agrees well with our data and especially with the data of Davies *et al.*³³

Eisenberg and LeTourneur¹⁴ have calculated the angular distribution for $\text{O}^{16}(\pi^-,nn)$ and $\text{O}^{16}(\pi^-,np)$ for

the two-nucleon capture mechanism and find satisfactory agreement with our preliminary data,³⁴ after taking into account the final-state interaction. Their curves for n - p emission are in fact slightly broader than their curves for n - n emission.

Cheon has made calculations⁷ for the $\text{C}^{12}(\pi^-,nn)\text{B}^{10}$ angular distribution which we compare with our O^{16} data in Fig. 10. He uses a two-nucleon correlation function of the type $f(r)=1-e^{-r^2}$ in a two-nucleon capture process. However, he makes the assumption that the two detected nucleons come out with equal energies. His curves for $\zeta_{pn}(^3S)=1.75$ F⁻² and $\zeta_{pn}(^3D)=1.8$ F⁻² are reproduced as the dotted curve in Fig. 10. One must conclude from the poor fit to the data that either the analyses for C^{12} and O^{16} are widely different, the approximation of equal energies is very poor, or other parts of the theory do not apply.

A calculation by Kolibasov¹² of the pion capture process on α -particle clusters reports the predominant role of this process over the two-nucleon capture process in the case $\text{O}^{16}(\pi^-,nn)$, by comparison with unpublished data of Ignatenko *et al.* However, our data do not support this conclusion. We see a predominant two-nucleon mechanism. The dash curve in Fig. 10 is Kolibasov's α -particle calculation and the dot-dashed curve in his two-nucleon process calculation. A moderate contribution of the α -particle capture process cannot be ruled out, however, since we do see some events even at small angles and the apparatus has discrimination against low-energy nucleons.

C. $W(n-n)/W(n-p)$ Ratio: R

The determination of the $W(n-n)/W(p-n)$ ratio involves first the definition of what is meant by correlated emission: the emission at exactly 180° , or that integrated over the entire peak near 180° . Also, it involved the absolute efficiency of the neutron and proton detectors and their solid angles as well as the number of coincidences recorded. The major source of possible systematic error is in the calculation of the neutron detector efficiency.

Statistical errors are typically only 10%, except in the case of Cu and Pb targets, where they are larger. Therefore, the over-all uncertainty is dominated by the possible systematic sources of error: about 25% for $W(p-n)$, 40% for $W(n-n)$, and 25% for the ratio. These are combined with the statistical errors in each case to give the errors quoted in Table I. The rates and ratios of Table I are those as measured by our apparatus. We have not made corrections by extrapolating to proton or neutron energies for which the apparatus is insensitive. In this sense the data may be biased for the kinematics of the two-nucleon capture process as opposed to a multinucleon capture process.

With respect to a definition of the ratio as the extrapolation of the angular distribution to 180° , or the integrals of the curves without the isotropic part, we

have done both but feel that the latter is a better measure to be compared to theories. The rates quoted in Table I are the integrals of the curves without the isotropic part. As previously mentioned, most of the p - n angular distributions are wider than the n - n distributions and the average factor by which they are wider is 1.5. Therefore, relatively more p - n coincidences are counted with an integration procedure and the ratio by integration is therefore lower. The weighted average of $W(n-n)/W(n-p)$ for p -shell nuclei is $R=3.3\pm 0.9$ by integration of the peaks and is $R=5.1\pm 1.6$ by extrapolation of the curves to 180° . The values obtained by integration of the peaks should be the ones compared to those obtained by Ozaki *et al.*³² since their detectors effectively integrated over most of the peak width. They obtained 5.0 ± 1.5 in C and 3.9 ± 1.2 in Al compared to our values of 2.5 ± 1.0 in C, 2.4 ± 0.9 in Al, and 3.3 ± 0.9 for the average of p -shell nuclei. Our values of R are uniformly lower.

We also used Cu and Pb targets to investigate whether a heavy nucleus gives a significantly different value of R . The values obtained, 2.0 ± 1.4 for Cu and 4.7 ± 4.7 for Pb, indicate that the ratio for heavy nuclei is about the same as for the p -shell nuclei within the large statistical errors associated with the measurements on the Cu and Pb targets.

Calculations of the ratio $R=W(n-n)/W(n-p)$ have been made by several theorists using various assumptions about various targets. These have most recently been summarized by Eisenberg and LeTourneur.¹⁴ A simple counting of p - p and n - p pairs within the nucleus with consideration of the Pauli principle gives a ratio of 3, which is in agreement with our measurement. However, Eisenberg and LeTourneur find that the final-state interaction greatly reduces this number. They predict R is less than 1. Also, they find that the initial two-nucleon correlations do not strongly influence the ratio.

Cheon¹⁷ has calculated for C^{12} the ratio as a function of the correlation parameters ζ_{pn} and ζ_{nn} described previously. Assuming $\zeta_{pn}=\zeta_{pp}$, our ratio of 3.3 ± 0.9 corresponds to $\zeta=1.57\pm 0.12 F^{-2}$ and our 180° value of 5.1 ± 1.6 corresponds to $\zeta=1.72\pm 0.13 F^{-2}$. Neither of these are unreasonable values of the correlation parameter but the same calculations did not fit our angular distributions on O^{16} . Cheon's calculation did not take into account the two-nucleon final-state interactions.

Jibuti and Kopaleishvili,⁸ and Kopaleishvili¹⁰ have considered the final-state interaction of the two outgoing nucleons and two-body correlations. They find that absorption on relative s -wave nucleons in the p shell gives a ratio greater than 1 whereas absorption on relative p -wave nucleons gives a ratio less than 1. Using a correlation function of the form

$$\begin{cases} 0, & r \leq r_c \\ 1 - e^{-\beta(r^2/r_c^2 - 1)}, & r > r_c \end{cases}$$

they obtain a ratio of 2.9 for C^{12} and 1.3 for O^{16} with the

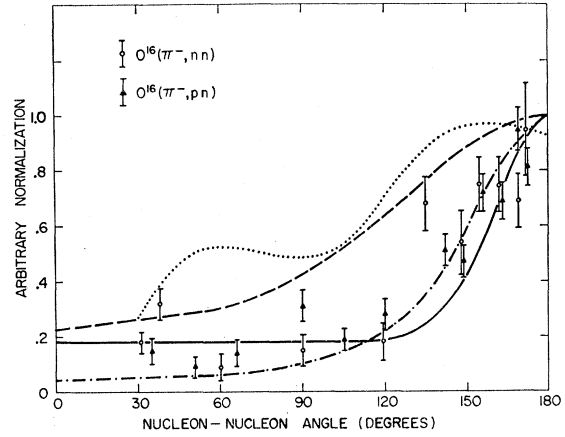


FIG. 10. Angular distributions from O^{16} compared with theories. All data and theories have been normalized to 1.0 at 180° . The solid curve is found in the same way as in Fig. 9, but with the parameters of O^{16} . The dotted curve is a calculation of Cheon (Ref. 17) for the two-nucleon mechanism. The dash curve is an α -particle cluster-model calculation of Kolibasov (Ref. 12) and the dot-dash curve is his calculation for the two-nucleon mechanism.

parameter $r_c=0.4 F$, but without a complete final-state interaction. With the final-state interaction, these ratios are reduced. In order to obtain a ratio as large as 4, they conclude that the proton-proton correlation within a nucleus must be weaker than the neutron-proton correlation. This conclusion may not be required to agree with our value of 3.3 ± 0.9 .

Kohmura⁹ has calculated the ratio R under the assumption that the pion is captured by a nucleon pair in a relative s -wave state, and he comes to the conclusion that R is 3 unless one allows charge-dependent nuclear wave functions. To obtain a ratio of 4 to 5 he must allow the range of a singlet s -wave pair to be longer by 5 to 10% than that of a triplet s -wave pair. This violates charge independence. Again, this conclusion may not be required to agree with our average value of 3.3 ± 0.9 . Kohmura uses a repulsive core to simulate the two-nucleon correlation but concludes that it does not change the ratio significantly. He does not include a final-state interaction.

Koltun and Reitan¹³ point out that a charge-exchange rescattering contribution which is generally neglected in other calculations is not negligible and tends to raise the value of R for O^{16} .

Aside from improving the accuracy of the ratio R in future experiments, two other questions remain to be answered. The first question concerns the sharpness of peaking of the n - n emission relative to the p - n emission. To be completely useful a theory must predict these widths and discuss whether a ratio obtained by integration over the peaks or by extrapolation of the peaks at 180° is the pertinent parameter. The second question is why all the nuclei measured have essentially the same value for the ratio. Perhaps in this experiment at least, capture on two nucleons in the s -shell core is as important as on the p -shell nucleons. In the case of Li^6 this

must be so since there are no p -shell p - p pairs. An experiment measuring complete kinematics could possibly settle this question.

Another approach to obtain the ratio R is to measure the ratio of emission of high-energy neutrons and protons. If these high-energy nucleons were produced only by the two-nucleon mechanism a measurement of the neutron rate would give $W(n-p)+W(n-n)$ and a measurement of the proton rate would give $W(n-p)$.³⁸ Our measurement of the high-energy proton spectrum indicates that, indeed, the major fraction of all high-energy protons are accompanied by a neutron and presumably produced by capture on two nucleons. Using the data of Fowler³¹ for protons and Anderson *et al.*³⁷ for neutrons, the high-energy rates are about in a ratio of 4, which implies $R=3$. Ammiraju and Lederman give a similar argument on the basis of measurements of charged particles only.²¹

D. Conclusions

The pulse-height spectra of protons in the two-nucleon emission following π^- absorption on C^{12} or O^{16} are in agreement with theory. The essential points of the theory considered are the kinematical constraints imposed by the two-nucleon emission mechanism and the approximation of shell-model wave function by an

³⁸ The neutron rate does not give twice $W(n-n)$ since the two neutrons are correlated in angle at 180° .

harmonic-oscillator approximation. The spectra are not sensitive to details in the nuclear structure of the target nuclei.

The angular distributions of the two emitted nucleons are closely fitted by any of several theories of a two-nucleon absorption process, while agreement with a multinucleon absorption process is poor. An average of 40% was measured for the branching ratio of π^- absorption yielding two correlated nucleons. An unexplained feature of the angular distribution is the observation that the n - p peaks at 180° are broader than the n - n peaks.

The ratio $R=W(n-n)/W(n-p)$ has been measured to be 3.3 ± 0.9 for the average of p -shell nuclei. This is in agreement with simple, incomplete theories ignoring the final-state interactions, and it is in agreement with other observations of single high-energy proton and neutron emission. More complete theories which include the final-state interactions predict a ratio of about 1. Clearly more detailed experiments and theories are called for to resolve this discrepancy.

ACKNOWLEDGMENTS

Conversations with Professor D. Koltun have been especially useful in clarifying many points in the analysis of this experiment. P. Lesser, T. Feit, and Miss T. Yang have been helpful in the collection and analysis of the data. We thank the 130-in. cyclotron staff for providing long hours of stable running conditions.